Motion of the sprung pendulum

M. G. Rusbridge
Department of Pure and Applied Physics, UMIST, Sackville Street, Manchester M60 1QD, United Kingdom
(Received 4 May 1979; accepted 21 August 1979)

We extend the analysis of the motion of the sprung pendulum to show the full effects of the nonlinear coupling between horizontal and vertical oscillations. We show that even at modest amplitudes a theory involving second-order terms only is inadequate to explain experimental results, and suggest that the discrepancy is due to nonlinear detuning from the exact resonance condition, an effect which appears only in higher order. Finally, we investigate the effect of damping on the patterns of motion.

I. INTRODUCTION

Cayton[1] has given an interesting description of the behavior of this simple mechanical system, a weight supported on a spring and free to move both horizontally and vertically. He was particularly interested in the parametric instability which leads to the growth of transverse oscillations when the weight is initially set into vertical motion. This is a fundamentally nonlinear effect, occurring when the vertical frequency is exactly twice the horizontal, and the system is among the simplest in which such effects can be demonstrated; it is also an analog of less accessible systems such as the frequency doubling of laser light in a nonlinear crystal.

In this paper I wish to point out that Cayton's analysis can be extended to give a more complete picture of the motion in the form of a set of trajectories in phase space. As Olsson[2] has shown, there are two steady-state modes of oscillation, which can indeed readily be demonstrated experimentally. However, in presenting some experimental results I shall show that they differ quantitatively from the theoretical predictions; computer simulations show that the difference is real and not an experimental artifact. These departures can plausibly be attributed to neglected higher-order terms, and in particular to nonlinear detuning of the 2:1 resonance condition; we shall show that the effects of a deliberate detuning are qualitatively similar to those observed. I have found that it is easy to forget that higher-order terms may be significant at what seem quite moderate amplitudes.

Falk[3] has also shown more rigorously that the trajectories should be closed, and has given expressions for the time variation of the amplitudes in terms of elliptic functions.

The detuning produces a characteristic distortion of the phase-space trajectories. We have also studied the effects of damping which can produce a different but equally characteristic distortion if the damping is small. However, if the damping rates of horizontal and vertical motions are different, and if the difference exceeds a certain limit dependent on the amplitude, the damping decouples the horizontal and vertical oscillations which decay away independently. If the damping rates are the same, the pattern of motion decays with no fundamental change. We have made some experimental observations which can be interpreted as being consistent with this result.

II. THEORY

We assume that the pendulum is constrained to move in a fixed vertical plane, and use Cartesian coordinates with origin at the equilibrium position of the weight (Fig. 1). It might seem more natural to use polar coordinates with origin at the point of suspension, as does Minorsky,[4] for example; however, the resulting equations are more complex and less transparent, while being, of course, exactly equivalent to those we shall derive.

From Fig. (1) we can write down the equations of motion in the form

$$m\ddot{x} = -T\sin\theta,$$
$$m\ddot{y} = T\cos\theta - mg,$$

where $T = \alpha(l - l_0')$ is the tension in the spring, α is the spring constant, and l_0' the unextended length of the spring. The length of the spring at equilibrium is given by $l = l_0$, where

$$\alpha(l_0 - l_0') = mg.$$

Substituting for T and mg in the equations of motion, and noting that $\sin\theta = x/l$ and $\cos\theta = (l_0 - y)/l$, we find

$$m\ddot{x} = -\alpha(l_0 - l_0')x/l,$$
$$m\ddot{y} = \alpha(l - l_0')(l_0 - y)/l - \alpha(l_0 - l_0'), \qquad (1)$$

where $l = [(l_0 - y)^2 + x^2]^{1/2}$ is the length of the spring. It is important to note that the nonlinearity arises purely from the geometry and not from the properties of the spring which is assumed linear. If we now substitute for l and expand the resulting equations to second order in x and y, we obtain

$$m\ddot{x} = -\alpha(1 - l_0'/l_0)x + \alpha(l_0'/l_0^2)xy,$$
$$m\ddot{y} = -\alpha y + (1/2)\alpha l_0' x^2/l_0^2. \qquad (2)$$

The linear terms give the fundamental frequencies

$$\omega_x^2 = (\alpha/m)(1 - l_0'/l_0),$$
$$\omega_y^2 = \alpha/m,$$

and our main interest is in the nonlinear resonance given by $\omega_y = 2\omega_x$; the condition for this is $l_0 = (4/3)l_0'$. In terms of these frequencies, Eqs. (2) become

 0002-9505/80/020146-06$00.50

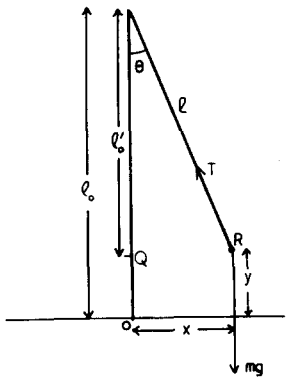

Fig. 1. Coordinate system and dimensions. O is the equilibrium position of the weight, and Q the position of the end of the spring with the weight removed. We use Cartesian coordinates with origin at O.

$$\ddot{x} = -\omega_x^2 x + \omega_y^2 l_0' xy/l_0^2, \tag{3}$$

$$\ddot{y} = -\omega_y^2 y + (1/2)\omega_y^2 l_0' x^2/l_0^2. \tag{4}$$

These equations have a simple interpretation in two limiting cases: when $x \ll y$ and y oscillates at its natural frequency

$$y = y_0 \cos(\omega_y t + \psi),$$

Eq. (3) becomes a Mathieu equation which for $\omega_y = 2\omega_x$ has solutions for x with exponentially growing amplitude; on the other hand, when $y \ll x$ and x oscillates at its natural frequency

$$x = x_0 \cos(\omega_x t + \phi),$$

Eq. (4) represents a forced simple harmonic motion (SHM), which for $\omega_y = 2\omega_x$ is driven resonantly, so that the solution for y has its amplitude increasing linearly with time. Taken together, these cases suggest a cyclic process in which energy is continually exchanged between the two modes of oscillation, and this solution is indeed well known.

We can find a more general solution by a straightforward application of the "stroboscopic" method.[4] We set

$$x = x_0(t)\cos[\omega_x t + \phi(t)], \tag{5}$$

$$y = y_0(t)\cos[\omega_y t + \psi(t)], \tag{6}$$

where x_0, y_0, ϕ, and ψ are slowly varying functions. Since there are now four unknown functions instead of two, we are free to introduce two further relations between them. We choose to set

$$\dot{x} \equiv -\omega_x x_0(t)\sin[\omega_x t + \phi(t)],$$

which requires that

$$\dot{x}_0 \cos(\omega_x t + \phi) - \dot{\phi} x_0 \sin(\omega_x y + \phi) = 0, \tag{7}$$

and similarly

$$\dot{y}_0 \cos(\omega_y t + \psi) - \dot{\psi} y_0 \sin(\omega_y t + \psi) = 0. \tag{8}$$

We also define the energy E_x by

$$E_x = (1/2)\dot{x}^2 + (1/2)\omega_x^2 x^2 \equiv (1/2)\omega_x^2 x_0^2,$$

so that Eq. (3) becomes

$$\frac{dE_x}{dt} = \omega_y^2 \frac{l_0'}{l_0^2} yx\dot{x}.$$

We substitute in this equation the expressions for x, y, and $\dot{x}$, and average over one complete cycle of the x oscillation assuming that the slowly varying functions are effectively constant. This yields

$$\frac{dE_x}{dt} = -\frac{1}{4}\frac{l_0'}{l_0^2}\omega_y^2 \omega_x x_0^2 y_0 \sin(2\phi - \psi), \tag{9}$$

and a similar procedure leads to

$$\frac{dE_y}{dt} = \frac{1}{4}\frac{l_0'}{l_0^2}\omega_y^2 \omega_x x_0^2 y_0 \sin(2\phi - \psi), \tag{10}$$

so that

$$\frac{dE_x}{dt} = -\frac{dE_y}{dt},$$

and the total energy $E_x + E_y$ is a constant of the motion of this order. Finally, Eqs. (9) and (10) suggest that it is useful to define $\theta = 2\phi - \psi$, and we obtain an expression for the rate of change $\dot{\theta} \equiv 2\dot{\phi} - \dot{\psi}$ from Eqs. (7) and (8); averaging this in the same way we obtain the result

$$\dot{\theta} = \frac{\omega_y^2 l_0'}{4 y_0 l_0^2}\left(\frac{1}{2}\frac{x_0^2}{\omega_y} - \frac{2y_0^2}{\omega_x}\right)\cos\theta. \tag{11}$$

In all these cases the average is over a time interval of $2\pi/\omega_x$. We now simplify Eqs. (9)–(11) by making explicit the relationships $l_0 = (4/3)l_0'$ and $\omega_y = 2\omega_x$; we also substitute for E_x, E_y in terms of x_0 and y_0, and finally express the equations in dimensionless variables

$$X = x_0/l_0, \quad Y = y_0/l_0, \quad \tau = \omega_x t.$$

These steps yield

$$\begin{aligned} \frac{dX}{d\tau} &= -\frac{3}{4}XY\sin\theta, \\ \frac{dY}{d\tau} &= \frac{3}{16}X^2\sin\theta, \\ \frac{d\theta}{d\tau} &= \frac{3}{8}\frac{(1/2)X^2 - 4Y^2}{Y}\cos\theta. \end{aligned} \tag{12}$$

The first two of these equations lead to

$$X^2 + 4Y^2 = \text{const} = X_0^2, \text{ say},$$

as an expression of the conservation of energy, and using this to eliminate Y we obtain

$$\frac{dX}{d\tau} = -\frac{3}{8}X(X_0^2 - X^2)^{1/2}\sin\theta, \tag{13}$$

$$\frac{d\theta}{d\tau} = \frac{3}{4}\frac{(3/2)X^2 - X_0^2}{(X_0^2 - X^2)^{1/2}}\cos\theta. \tag{14}$$

The motion can therefore be represented by trajectories in the (X,θ) plane, which satisfy the equation

$$\frac{dX}{d\theta} = -\frac{1}{2}X\frac{X_0^2 - X^2}{(3/2)X^2 - X_0^2}\tan\theta,$$

which can be integrated to yield

$$X^2(X_0^2 - X^2)^{1/2}\cos\theta = \text{const}, \tag{15}$$

C say, so that the trajectories form closed loops; C is an additional constant of the motion. The trajectories are shown in Fig. 2. There are two degenerate trajectories consisting of the equilibrium points $X = [(2/3)X_0]^{1/2}$, $\theta = 0$ or π, which represent steady-state oscillations; all other trajectories involve the cyclic transfer of energy between the two fundamental oscillations, and for $C = 0$ we have a

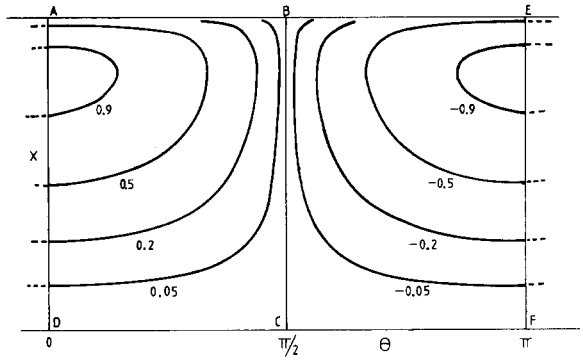

Fig. 2. Predicted trajectories in (X,θ) from Eq. (15). Half of each trajectory is shown; it is completed by its mirror image in *AB* or *EF*. Each is labeled by the value of C normalized to its maximum value $(2/3\sqrt{3})X_0^3$. The limiting trajectory $C = 0$ giving complete transfer is represented by ABCD (or EBCF, which is indistinguishable).

limiting trajectory in which the transfer is complete: this is represented by the rectangles ABCD or EBCF in Fig. 2. It is readily shown that these limiting trajectories are traversed only in infinite time, since for $X \ll X_0$, $\sin\theta = 1$, Eq. (13) gives

$$\frac{dX}{d\tau} = -\frac{3}{8}XX_0,$$

$$X \propto \exp(-(3/8)X_0\tau),$$

and the point C is approached but never reached. Trajectories in the neighborhood of the equilibrium points can be followed explicitly by linearizing Eqs. (13) and (14) about these points: this is straightforward and shows that small closed loops are traversed in a time

$$\tau_0 = 8\pi/3X_0;$$

the dependence on X_0 being exactly as expected for a second-order nonlinear process.

In the terminology of Minorsky[4] the equilibrium points are "centers"; the corners of the rectangles forming the limiting trajectory are "saddle points." (I use the term "limiting trajectory" loosely: strictly we have four separate trajectories for $C = 0$, forming the four sides of the rectangle, but complete trajectories lie only infinitesimally far away from them, and in fact, we anticipate that higher-order effects will ensure that even the limiting trajectory can be traversed in a finite time.)

At the equilibrium points the amplitudes are in the ratio

$$y_0/x_0 \equiv Y/X = 1/2\sqrt{2}\,.$$

The motion in the (x,y) plane at equilibrium traces out parabolas

$$y/y_0 = \pm\,(1 - 2x^2/x_0^2),$$

the sign being negative for $\theta = 0$ and positive for $\theta = \pi$.

III. EXPERIMENT AND COMPUTATION

The general features of the predicted motion, including the existence of the equilibrium points and the cyclic trajectories, have been confirmed with several pendulums constructed by different students. In the case to be described, the pendulum was 38 cm long when weighted at resonance: the weight consisted largely of a battery and light bulb which was (fortuitously) very nearly the required weight for resonance. Thus the motion in physical space could be recorded straightforwardly on film. Some typical results are shown in Fig. 3. There was little tendency in this case for the plane containing the motion to rotate. (This was not always the case, and some pendulums seem very bad in this respect for no very obvious reason. In the bad cases, deliberate attempts to remove the degeneracy of the horizontal oscillations, as, for example, by designing the pivot to facilitate swinging in one plane, have proved rather ineffective.)

The main experiment with this pendulum was to investigate how the time for one complete cycle varied with initial conditions. The pendulum was released from rest at different values of x and y (which thereby define initial amplitudes x_0 and y_0 at $t = 0$), and the cycle time measured as a function of x_0 and y_0. The results are shown as a contour diagram in Fig. 4.

In this diagram, the dimensionless amplitude X_0 is constant along ellipses $x_0^2 + 4y_0^2 = \text{const}$. On every such curve we expect the cycle times to reach a maximum (in principle infinite) for $x_0 = 0$ and for $y_0 = 0$. In fact, as can be seen from Fig. 4, maximum cycle times are found for $x_0 = 0$ and on a curve $y_0 = x_0^2/2l_0$, which represents approximately the track of a pendulum of *fixed* length l_0.

It is apparent that this result could not be reproduced by the theory of Sec. II, since there x_0 and y_0 are taken to be quantities of the same order. However, before discussing it as a higher-order effect we shall present the results of a computational simulation, which confirm that the effect is not due to any experimental artifact.

These computations were carried out using a fifth-order

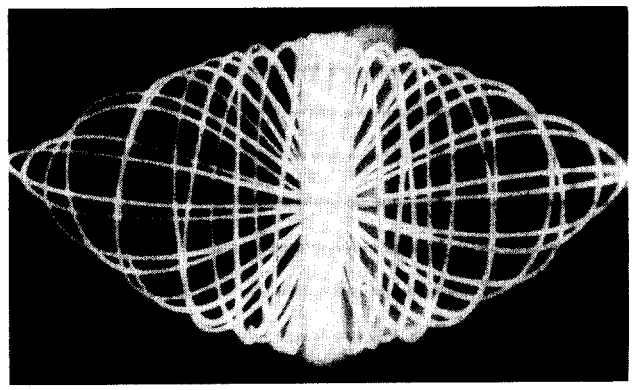

(a)

(b)

Fig. 3. Typical patterns (in physical space) generated by the pendulum weight for different initial conditions: (a) near the limiting trajectory; and (b) near an equilibrium point.

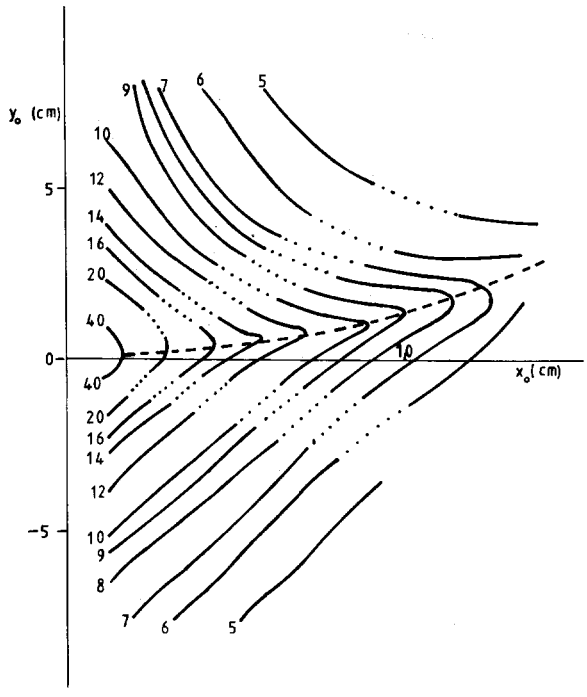

Fig. 4. The cycle time measured experimentally as a function of the initial displacements X_0, Y_0 for a pendulum of length 38 cm when stationary. The results are plotted as a contour diagram with contours labeled with the cycle time in seconds. The dotted portions represent regions near the equilibrium points where very little change in the pattern occurs and accurate values of the cycle time cannot be measured. The dashed curve is the path of a pendulum of fixed length.

Runge–Kutta process to solve Eqs. (1) directly; the code[5] was an adaptation of one developed for following trajectories of charged particles in magnetic fields, and is sufficiently accurate to conserve the total energy to within 1 part in 10^8 per step. Trajectories were followed for a variety of initial conditions consistent with a constant value of $X_0 = 0.117$, typical of experimental amplitudes. Some typical results are shown plotted as trajectories in the (X,θ) plane in Fig. 5. To obtain these results from the computed values of x, $\dot{x}$, y, and $\dot{y}$ the phase was defined at each instant by

$$\phi = \tan^{-1}(\dot{x}/\omega_x x),$$
$$\psi = \tan^{-1}(\dot{y}/\omega_y y),$$
$$\theta = 2\phi - \psi.$$

Thus the oscillations of the phase apparent in Fig. 5 are a measure of the breakdown of the assumption of slowly varying phase in Eqs. (5) and (6). Each trajectory in effect fills a band in the (X,θ) plane. The bands appear to close on themselves, however, and we have so far observed no tendency for the trajectories to become stochastic. Thus there exists a constant of the motion other than the energy, although it cannot be given exactly by Eq. (15).

The pattern shown in Fig. (5) resembles that in Fig. (2) but with significant differences. The trajectory marked L in Fig. (5) has initial conditions $X = X_0$, $Y = 0$, $\theta = 0$, which according to Sec. II should define the limiting trajectory, but it clearly follows a very different path. There is a band of trajectories which are not closed since θ changes monotonically with time (at least when the fast oscillations are smoothed out), and the equilibrium positions are not symmetrical but are displaced from the predicted value of $X = [(2/3)X_0]^{1/2} = 0.095$.

To show that these departures have essentially the same significance as those observed experimentally, we plot in Fig. 6 the cycle time τ_0 as a function of the initial value of Y. Clearly these results are also consistent with a maximum at $Y \simeq (1/2)X^2$, equivalent to the result obtained from experiment, rather than at $Y = 0$ as the simple theory suggests.

We conclude that the departures from the theory of Sec. II are indeed due to higher-order terms in the expansion. We have not attempted to develop the theory to higher order; instead, in Sec. IV it will be shown that the results in Fig. 5 are qualitatively similar to those obtained when the pendulum is detuned slightly from resonance. Accordingly we suggest that the most important higher-order effect is a change in the average length of the pendulum leading to an effective nonlinear shift in the resonance condition and thus to a detuning of a pendulum which at rest satisfies the condition for resonance.

IV. MOTION OFF EXACT RESONANCE

If we assume that the resonance condition is not exactly met we can write

$$2\omega_x = \omega_y + \delta\omega$$

or

$$\omega_y/\omega_x = 2 - \Delta,$$

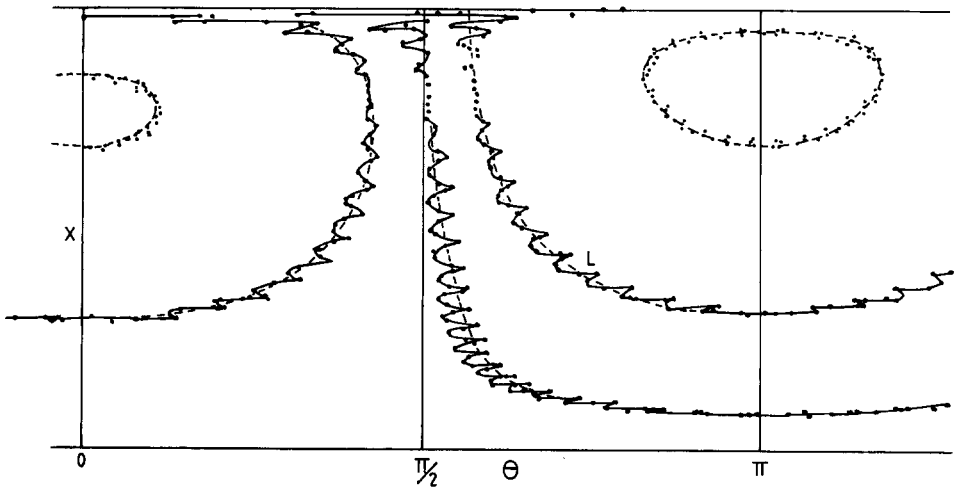

Fig. 5. Trajectories in (X,θ) generated by a computational simulation based on Eqs. (1). Plotted points are taken from the computer printout and are joined up into a continuous curve where possible. The dashed lines are smoothed versions for comparison with Figs. 2 and 7.

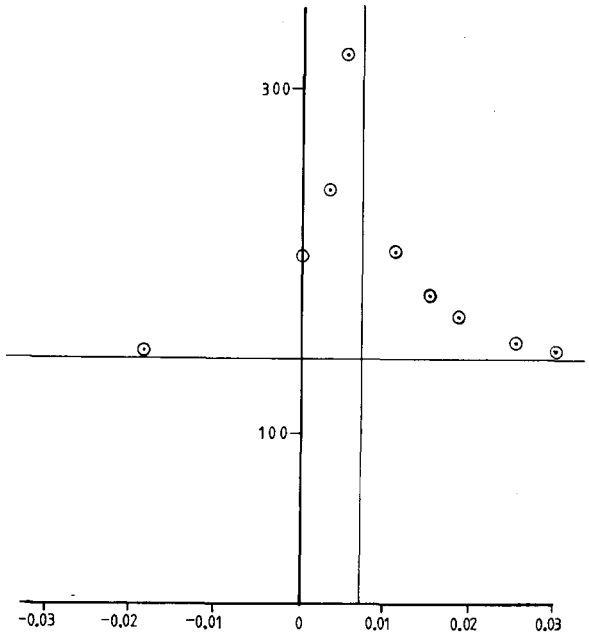

Fig. 6. The cycle time τ_0 as a function of Y_i for fixed $X_0 = 0.117$. The verticle line indicates the value $Y_i = 0.0068$ given by the expression $Y = (1/2)X^2$; the horizontal line indicates the value $\tau_0 = 143$ given by the expression $\tau_0 = 8\pi/3X_0$ for the cycle time near equilibrium.

say, where $\Delta = \delta\omega/\omega_x$ is a measure of the detuning. The length ratio is then

$$l_0' = 1 - 1/(2-\Delta)^2 \simeq (3-\Delta)/4$$

for small Δ. The development given in Sec. II goes through unchanged as far as Eqs. (9) and (10) except that the phase $2\phi - \psi$ is replaced by $2\phi - \psi + \delta\omega t$. We now substitute the expressions for ω_y/ω_x and l_0'/l_0 given above and change to dimensionless variables to obtain the following equations which replace Eq. (12):

$$\frac{dX}{d\tau} = -\frac{3}{4}\left(1 - \frac{\Delta}{2}\right)XY\sin(\theta + \Delta\tau),$$

$$\frac{dY}{d\tau} = \frac{3}{16}X^2\sin(\theta + \Delta\tau), \tag{16}$$

$$\frac{d\theta}{d\tau} = \frac{3}{8}\left(1 - \frac{\Delta}{2}\right)\frac{(1/2)X^2 - 4(1-\Delta/2)Y^2}{Y} \times \cos(\theta + \Delta\tau).$$

The constant of the motion X_0 is now given by

$$X_0^2 = X^2 + 4(1 - \Delta/2)Y^2.$$

These expressions are exact, but we shall now assume $\Delta \ll 1$, and define

$$\theta' = \theta + \Delta\tau. \tag{17}$$

Eliminating Y in terms of X and X_0 as before, we obtain

$$\frac{dX}{d\tau} = -\frac{3}{8}X(X_0^2 - X^2)^{1/2}\sin\theta', \tag{18}$$

$$\frac{d\theta'}{d\tau} = \Delta + \frac{3}{8}\frac{3X^2 - 2X_0^2}{(X_0^2 - X^2)^{1/2}}\cos\theta'. \tag{19}$$

Although these equations are not immediately separable, the trajectories can still be expressed in terms of a constant of the motion in the form

$$X^2(X_0^2 - X^2)^{1/2}\cos\theta' + (4/3)\Delta(X_0^2 - X^2) = \text{const} = C_\Delta, \text{ say.} \tag{20}$$

We show in Fig. 7 a set of trajectories obtained for different values of C_Δ for $X_0 = 0.117$ and $\Delta = 0.01$; the main features qualitatively reproduce those of Fig. 5. The equilibrium points are now located at $\theta' = 0$, $X = [(2/3)X_0]^{1/2} - \epsilon$, and $\theta' = \pi$, $X = [(2/3)X_0]^{1/2} + \epsilon$, where $\epsilon = (2\sqrt{2}/9)\Delta$, and it can easily be verified that they remain centers.

From Eq. (17) above, a constant θ' implies a continuously changing phase θ, and this in turn implies a change in the oscillation frequencies. The change is, in fact, exactly that required to cancel the detuning: if we define effective frequencies ω_x', ω_y' by

$$\omega_x' = \omega_x + \dot{\phi}, \quad \omega_y' = \omega_y + \dot{\psi},$$

then

$$2\omega_x' - \omega_y' = 2\omega_x - \omega_y + \dot{\theta} = \omega_x\left(\Delta + \frac{d\theta}{d\tau}\right) = \omega_x\frac{d\theta'}{d\tau} = 0.$$

This is an example of nonlinear entrainment.[4]

We suggest that the similarities between the patterns shown in Figs. 5 and 7 show that the departures from the simple theory are due to detuning resulting from higher-order terms. We would not expect exact agreement between Figs. 5 and 7 since the effective mean length and hence the detuning will vary during a cycle.

V. EFFECT OF DAMPING

Minorsky[2] has pointed out that a center is usually a marginal type of equilibrium point, separating stable from unstable foci (near which the trajectories spiral towards, or away from, the actual equilibrium point). Thus where an equilibrium point appears to be a center, it is likely that a more realistic physical description will, in general, reveal it to be properly a focus. The system under discussion illustrates this point, as we shall show by including the effects of damping. We assume that the damping is linear, but we allow different damping constants λ_x and λ_y for the horizontal and vertical oscillations, respectively. We also assume that the damping is small, λ_x, $\lambda_y \ll \omega_x$. For the sake of simplicity we consider only exact resonance $\omega_y = 2\omega_x$. The

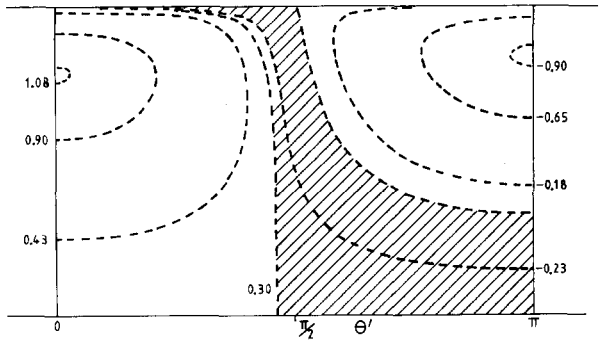

Fig. 7. Predicted trajectories in (X,θ') from Eq. (20) for a detuned pendulum with $\Delta = 0.01$, $X_0 = 0.117$. Trajectories are labeled by the value of C_Δ, normalized in the same way as in Fig. 2. The shaded region contains open trajectories. As in Fig. 2, trajectories are completed by reflection in $\theta' = 0$ or π as appropriate.

development exactly parallels that in Sec. II and leads to the equations

$$\frac{dX}{d\tau} = -\frac{3}{4}XY\sin\theta - \frac{1}{2}\Lambda_1 X,$$
$$\frac{dY}{d\tau} = \frac{3}{16}X^2\sin\theta - \frac{1}{2}\Lambda_2 Y, \qquad (21)$$
$$\frac{d\theta}{d\tau} = \frac{3}{8}\frac{(1/2)X^2 - 4Y^2}{Y}\cos\theta,$$

where $\Lambda_1 = \lambda_x/\omega_x$, $\Lambda_2 = \lambda_y/\omega_x$. These equations have an obvious interpretation, and it is physically reasonable that the equation for the phase should be unaltered by including the damping.

Now, of course, X_0 is no longer a constant of the motion, and we have to disentangle changes in the pattern of motion as shown in Fig. 2 from changes simply in the amplitude. We note that X_0 determines only the vertical scale of Fig. 2 (and the time taken to traverse the trajectories), but not the shapes of the trajectories themselves: we can eliminate the effects of changes in amplitude by defining new variables $W = X/X_0$, $V = Y/X_0$. Some tedious algebra then leads to the pair of equations

$$\frac{dW}{d\tau} = -\frac{3}{8}W(1 - W^2)^{1/2}X_0\sin\theta - (\Lambda_1 - \Lambda_2)W(1 - W^2), \qquad (22)$$

$$\frac{d\theta}{d\tau} = \frac{3}{4}\frac{(3/2)W^2 - 1}{(1 - W^2)^{1/2}}X_0\cos\theta. \qquad (23)$$

One result follows immediately: if the damping constants are equal then these equations become formally identical with Eqs. (13) and (14), and the pattern of motion is unchanged. For the case $\Lambda_1 \neq \Lambda_2$ we confine ourselves to discussing the stability of the equilibrium points. We first note that, in general, they are shifted from the undamped positions: setting simultaneously $d\theta/d\tau = 0$, $dW/d\tau = 0$, we find from Eq. (23) that $W = (2/3)^{1/2}$ as before (ignoring the possibility $\cos\theta = 0$ which leads to the saddle points) and substituting the value in Eq. (21), we find

$$\sin\theta = -(8/3\sqrt{3})(\Lambda_1 - \Lambda_2)/X_0. \qquad (24)$$

Thus the displacement of the equilibrium points is orthogonal to that produced by detuning. We note that these equilibria exist only for large enough amplitude

$$X_0 > (8/3\sqrt{3})|\Lambda_1 - \Lambda_2|. \qquad (25)$$

We now linearize about these equilibrium points, with the anticipated result that trajectories around these points are no longer closed loops but spiral outwards or inwards, corresponding to an unstable or a stable focus, for $\Lambda_1 - \Lambda_2 > 0$ or < 0. In the former case, the expanding trajectories must eventually converge onto the limiting trajectory for $C = 0$ discussed in Sec. II. This result has a simple physical interpretation: in this limiting trajectory the system spends far more time oscillating nearly vertically with $Y > X$ than vice versa, so that by moving towards this trajectory the system minimizes the time it spends in the more highly damped mode. Conversely, for $\Lambda_1 < \Lambda_2$ the system will attempt to maximize the contribution of the horizontal mode to the motion, and this is achieved by moving towards the equilibrium points.

Finally, we consider briefly what happens when condition (25) is not longer satisfied; eventually, this must happen since X_0 is decreasing with time. The two equilibrium points then come together and vanish: at the same time, the saddle points become nodes and the system moves towards either $X = 0$ (pure vertical oscillation) if $\Lambda_1 > \Lambda_2$, or $X = X_0$ (pure horizontal oscillation) if $\Lambda_1 < \Lambda_2$. Thus for X_0 less than the limit set by Eq. (25), the two oscillations are effectively decoupled by the damping, and after some time only the more slowly damped oscillation will remain.

These results have not been tested by experiment in any detail. We have carried out one set of measurements, however, in which we noted that changes of the trajectory would be reflected in changes of the patterns of photographic records such as those of Fig. 3. Accordingly, we set a pendulum swinging, exposed films for one complete cycle at several different times during the lifetime of the motion, and looked for changes in the shape of the pattern. We found no evidence for any changes; all dimensions of the pattern diminished with time in strict proportion within experimental error. The values of λ_x and λ_y were not measured, but with a roughly spherical weight and air resistance the main source of damping it is quite plausible that $\Lambda_1 \simeq \Lambda_2$ in this experiment. In the future we plan to carry out experiments in which the damping constants are deliberately made different (e.g., by the use of vanes attached to the weight).

VI. CONCLUSIONS

The sprung pendulum is a simple mechanical device exhibiting a variety of nonlinear phenomena. It has already been discussed as an example of parametric instability; we have extended the analysis which leads to this to display the complete range of motion. However, comparison with experiment and computer simulations show that at modest amplitudes second-order theory is inadequate to explain the details of the motion. We have suggested that the important higher-order effect is detuning caused by a change in the mean length, and have shown that deliberate detuning will reproduce the observed pattern of trajectories at least qualitatively. We have discussed the effects of damping on the pattern of trajectories and have shown, in particular, that there is no effect if the damping of horizontal and vertical motions is the same. Some limited experimental evidence is consistent with this. Finally, we have shown that for unequal damping constants the changes in pattern have a simple physical interpretation.

ACKNOWLEDGMENTS

The experimental and some of the computational work has been undertaken by a succession of final year undergraduate students in the Department of Pure and Applied Physics of UMIST. Particular contributions have been made by R. Sheldrake (Sec. III), M. Yarwood (Sec. V), and G. Mitropoulos (Sec. V).

[1] T. E. Cayton, Am. J. Phys. **45**, 723 (1977).
[2] M. G. Olsson, Am. J. Phys. **44**, 1211 (1976).
[3] L. Falk, Am. J. Phys. **46**, 1120 (1978).
[4] N. Minorsky, *Nonlinear Oscillations* (Van Nostrand, New York, 1962).
[5] M. G. Rusbridge, Plasma Phys. **13**, 977 (1971).